SURFACE DAMAGE AND EFFECTS OF HEAT TREATMENT ON LARGE GRAIN Nb CAVITIES*

D. Kang, T.R. Bieler#, Michigan State University, East Lansing, MI 48824, U.S.A.
C. Compton, Facility for Rare Isotope Beams, East Lansing, MI 48824, U.S.A.

Abstract

Large grain Nb is being investigated for fabricating superconducting radiofrequency (SRF) cavities as an alternative to the traditional approach using fine grain Nb sheet. Past studies have identified a surface damage layer on fine grain cavities due to deep drawing and demonstrated the necessity for chemical etching on the surface. However, the underlying origin and mechanisms for the damage layer are not well understood, and similar exploration on large grain cavities is scarce. In this work, electron backscattered diffraction (EBSD) is used to examine the cross-sections at the equator and iris of a half-cell deep drawn from large grain Nb. Results indicate that the damage depends on crystal orientations, is different at the equator and iris, and is sometimes present through the full thickness of a cavity. After EBSD, the specimens were heat treated at 800 ºC and 1000 ºC, and the same areas were examined again for the effects of heat treatment on healing of the damage layer. Different responses were observed at the iris and equator despite the same annealing schedule.

INTRODUCTION

High purity Nb has been used to fabricate superconducting radiofrequency (SRF) cavities for particle accelerators over the past couple decades. SRF cavities can be formed by deep drawing slices directly cut from Nb ingots with large grains, as an alternative to the well-established technique using rolled fine grain Nb. Thus far similar accelerating gradients have been achieved from both approaches, although the reproducibility for large grain cavities is not yet well established. Large grain Nb slices have less uniform formability compared to fine grain Nb sheets, which leads to problems such as thickness variations and ridges at grain boundaries in deep drawing, and can affect cavity performance. There is an ongoing debate in the SRF community as to whether the cost savings from eliminating the rolling steps justify the potentially less predictable manufacturing and performance characteristics of large grain cavities [1, 2].

The deformation behavior of large grain Nb in deep drawing is complicated and current understanding is preliminary. Baars *et al.* made initial progresses in this direction by studying uniaxial tensile deformation of Nb single crystals [3]. A related and less complex issue is the surface damage due to the friction effects from the die in deep drawing. Kneisel *et al.* identified the dependence of achievable accelerating gradients on the amount of material removed from cavity surface [2, 4] (Fig. 1). The thickness for the surface damage layer was estimated to be 100~200 µm. Therefore, removing surface material from deep drawn cavities by chemical processing has become normative for the SRF community. However, the underlying mechanisms for surface damage have yet to be sufficiently explored. Besides, the analysis was done on fine grain cavities, and it is of interest as to whether large grain cavities require a similar amount of damage layer removal in response to deep drawing.

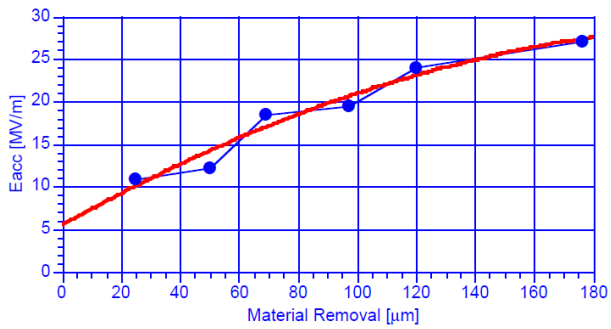

Figure 1: Dependence of achievable gradients on the amount of material removed from cavity surface [4].

Another fabrication routine for SRF cavities is a heat treatment following deep drawing. Various heat treatment schedules have been conducted in the SRF community [5], such as 600 °C for 10 hours, 800 °C for two hours, and 1000 °C for two hours, and no consensus has been reached as to which one is the most beneficial for cavity performance. While it is commonly understood that heat treatments eliminate dislocations by mechanisms of recovery and recrystallization, it is desirable to obtain a more quantitative and mechanistic understanding about how many dislocations can be removed. Also, Chandrasekaran *et al.* found that a heat treatment temperature above 800 °C contributes to the recovery of phonon peaks on single crystal and bi-crystal specimens, especially for the strained samples [6, 7]. This implies that a higher annealing temperature may be necessary for large grain cavities. To examine this, the specimens were heat treated at 800 °C and 1000 °C for two hours and characterized again after the heat treatment.

* The author would like to thank G. Ciovati and G.R. Myneni from Jefferson Lab for supplying the samples used in this work. The work was supported by the U.S. Department of Energy, Office of High Energy Physics, through Grant No. DE-S0004222.
#bieler@egr.msu.edu

ISBN 978-3-95450-143-4

Dislocations in a crystalline material exist in two forms [8, 9]. Geometrically necessary dislocations (GND) account for the lattice curvature, which is a slight change of crystal orientations within a grain. Such orientation gradients can be revealed by plotting a local average misorientation (LAM) map, in which larger LAMs typically correspond to higher GND content. Statistically stored dislocations (SSD) are slightly displaced dislocation pairs of opposite sign that do not contribute to the net orientation gradient. SSDs mainly result from dislocations being randomly trapped during plastic deformation, and when there are adequate driving forces (e.g. elevated temperature), neighboring SSDs with opposite signs can move towards each other and annihilate themselves.

Romanenko identified a correlation between LAMs and "cold" and "hot" regions of a large grain cavity, where higher LAMs correspond to hot regions [10]. The temperature increase from local heating increases the fraction of normally conducting electrons, which can cause thermal instabilities that locally degrade the superconducting state, so any potential sources for the heating need to be minimized. A proposed explanation for the local heating is that the vibration of dislocation lines interferes with heat transfer [1]. Dislocations can affect cavity performance if they pin magnetic flux centers, resulting in the irreversibility of magnetization curves (energy loss during a cycle) [2]. These adverse effects of dislocations necessitate a heat treatment for recovery/recrystallization after deep drawing.

MATERIALS AND METHODS

This study used excess material removed from the equator and iris of a large grain cavity prepared by Jefferson Lab. Two rings of excess material were first trimmed off the equator and iris, using electron discharge machining (EDM). Then two specimens were extracted from the equator ring, and another one from the iris ring, as shown in Figure 2. All three specimens contained a grain boundary and geometrical earing (heterogeneous deformation) features associated with the grain boundary. The cross sections of the specimens were hand ground with sandpaper to remove the EDM recast layer. After a final round using 4000 grit sandpaper with a particle size of about 3 µm, the specimens were given a light chemical etching that removed another 10 µm material from the surface to provide a surface suitable for electron backscattered diffraction (EBSD) analysis using a scanning electron microscope [11]. In this study, an 800 °C/2hr heat treatment was given to the iris specimen, and the two equator specimens were heat treated at 800 °C/2hr and 1000 °C/2hr.

Various analyses can be performed using an EBSD dataset, one of which is based upon the LAM method. For a given data point, the LAM reports the average misorientations between all of its neighboring points surrounding a specified kernel. Figure 3 illustrates a LAM calculation using the 2nd nearest neighbor sampling

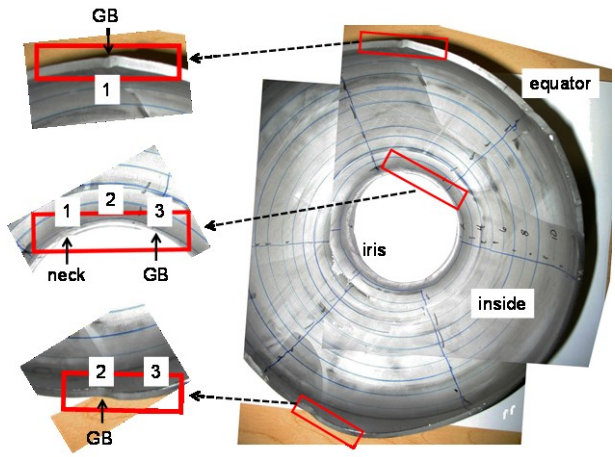

Figure 2: Locations where the three specimens were extracted from a half cell provided by Jefferson Lab. Grain boundaries (GB) and a neck are indicated in the blown-up images on the left. Numbers mark roughly where each EBSD scan was done on the equator/iris (in cross reference with Fig. 4). As a convention, the concave side is the inside of a cavity, and the opposite being the outside.

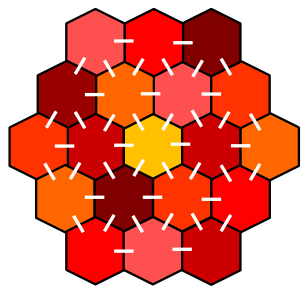

Figure 3: LAM calculations using the 2nd nearest neighbor sampling area (for the point at the center, average the misorientations between all of its neighboring points connected by the short white lines surrounding the kernel) [12].

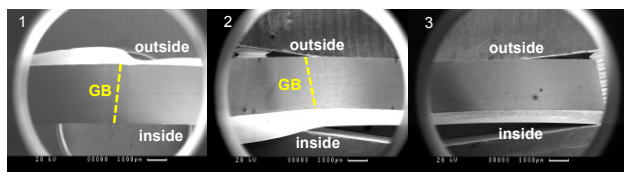

Areas (cross sections) scanned on the equator specimens

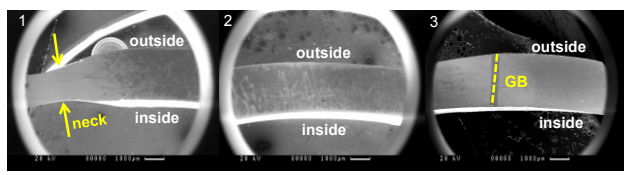

Areas (cross sections) scanned on the iris specimen

Figure 4: Secondary electron images for the 6 cross-sectional areas examined by EBSD. Grain boundaries and the neck are marked in accordance with Fig. 2. The numbering is also the same as Fig. 2.

area [12]. For the point at the center, the LAM assesses all the point pairs connected by the short white lines.

LAM results can be presented in the form of a colored map or a histogram. In an LAM colored map, each EBSD data point is assigned a color from blue to red, corresponding to misorientations from 0 ° to a maximum (user defined). Misorientations that are greater than the maximum are white. In an LAM histogram, the angular range of misorientations is divided into small user defined bins, and the number of misorientations contained in each bin is counted, which determines the number fraction for each bin.

RESULTS AND DISCUSSION

Figure 4 shows the secondary electron images for the 6 cross-sectional areas where the EBSD scans were

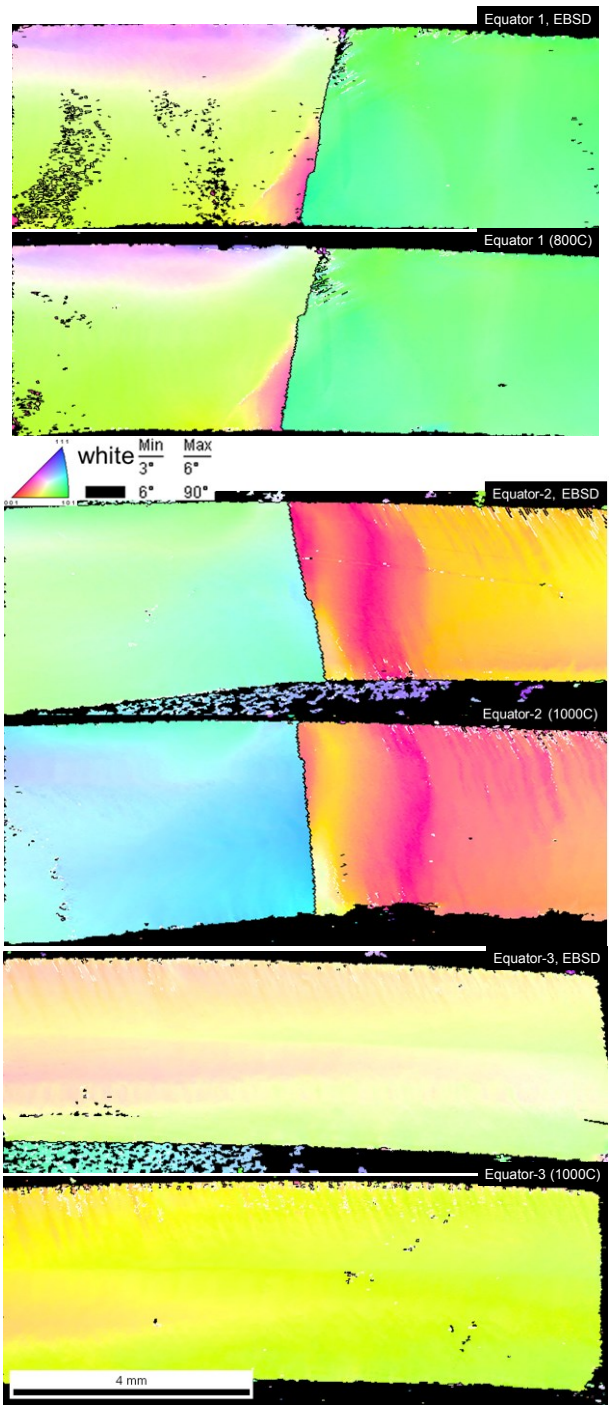

Figure 5: Normal direction orientation maps for the three equator scans (scale and legend are shared), before and after heat treatment (800 °C or 1000 °C for two hours). Grain boundaries are marked by black (>6 °) or white (3~6 °).

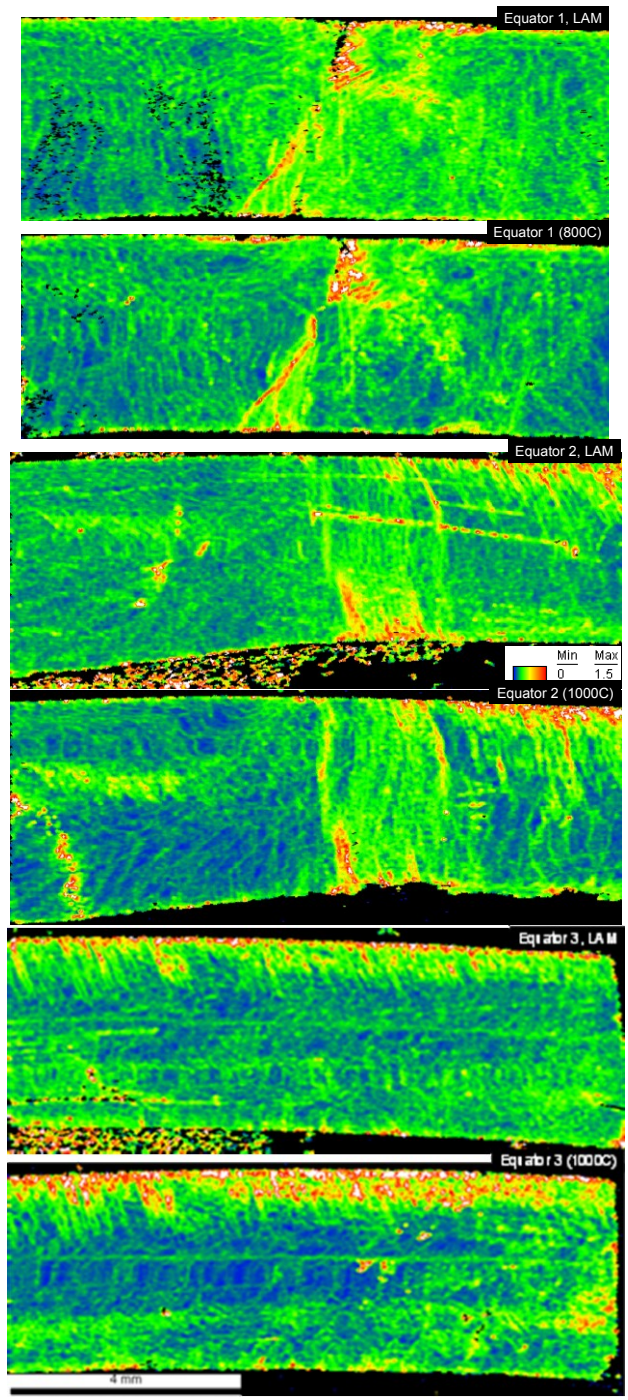

Figure 6: LAM maps for the three equator scans (scale and legend are shared), before and after heat treatment (800 °C or 1000 °C for two hours). A color from blue to red represents a misorientation from 0 ° to 1.5 °.

ISBN 978-3-95450-143-4

performed. The specimens were mounted such that the outside of the cavity (convex side) always faced upwards. A step size of 20 µm was used for each scan. Normal direction orientation maps and LAM maps are shown in Figures 5-8 for the equator and iris. For a better visualization of the effects of heat treatment, orientation and LAM maps from matching areas before and after heat treatment are shown above and below each other as a pair.

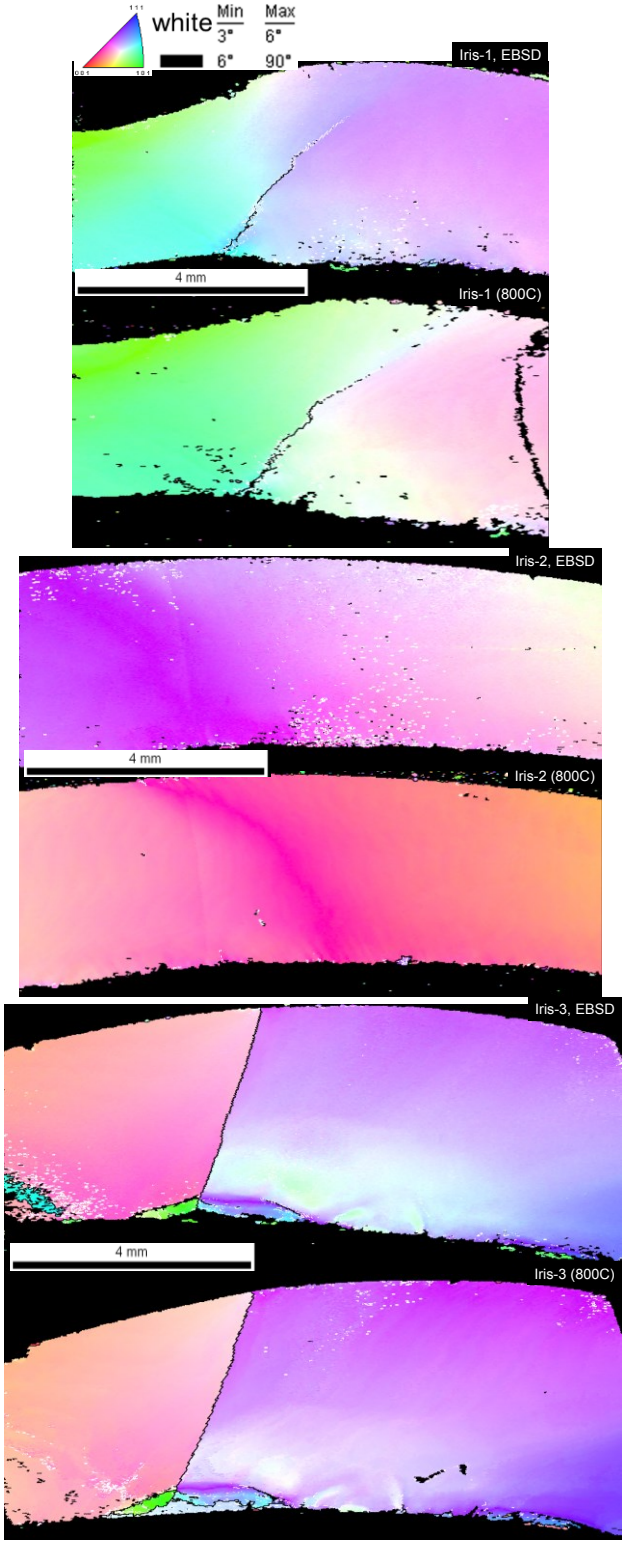

Figure 7: Normal direction orientation maps for the three iris scans (scale and legend are shared), before and after heat treatment (800 °C for two hours). Grain boundaries are marked by black (>6 °) or white (3~6 °).

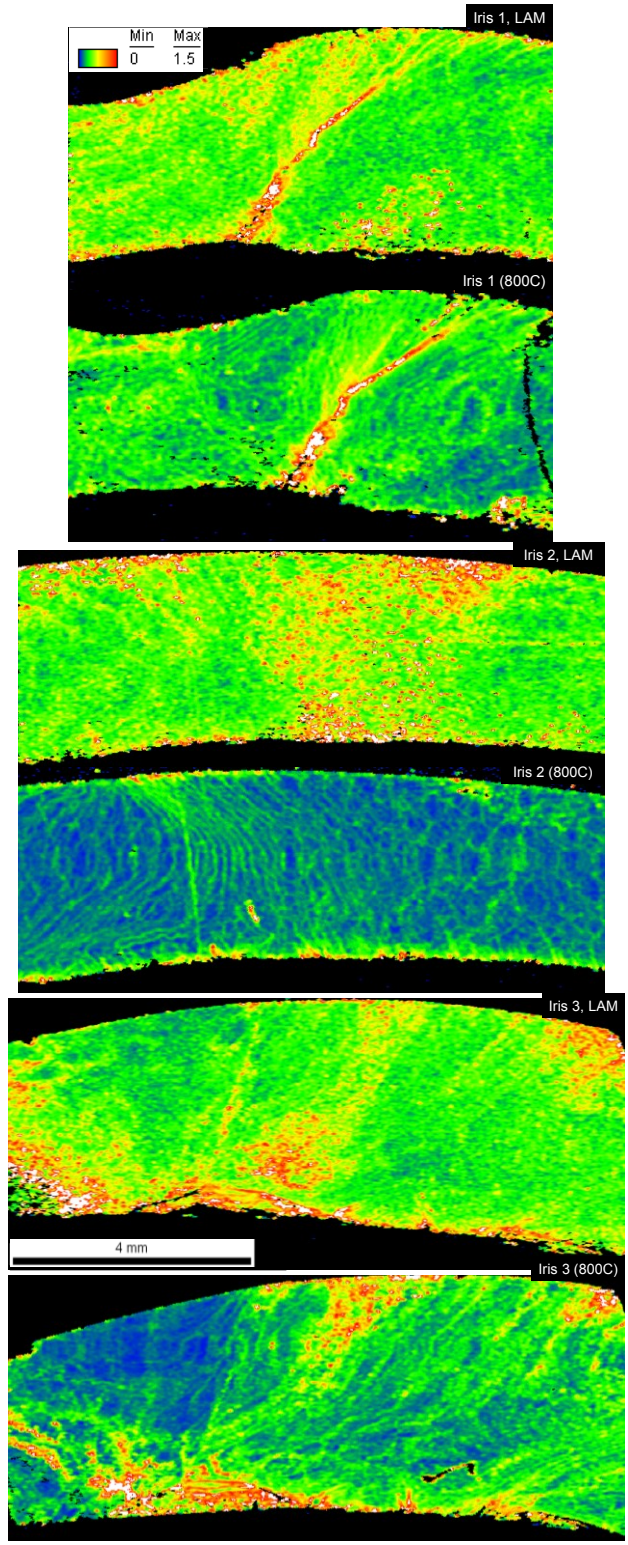

Figure 8: LAM maps for the three iris scans (scale and legend are shared), before and after heat treatment (800 °C for two hours).

The LAM maps are shown using the 2nd nearest neighbor sampling area and a color scale from blue (0°) to red (1.5°). The red and white color near the surface indicates larger local average misorientations than the blue and green in the bulk, which is evidence for surface damage.

LAMs are dependent on grain orientations. For example, the second pair in Fig. 6 (equator 2) shows that LAM values on the outer surface are greater in the right grain than in the left, and the difference is even bigger after heat treatment. The heat treatment reduced the magnitude of orientation gradients inside the material, as the color became a stronger blue, which represents a more perfect crystal. However, it did not change orientation gradients on the surface. The high LAM values vary in depth from 50 to 200 μm, similar to the amount of material that is commonly removed by etching from the inside of the cavity. Also, a comparison between the equator and iris in Figs. 6 and 8 reveals that the iris underwent a more severe deformation than the equator. Prior to heat treatment, the equator scans have large areas that are blue, while the iris scans are dominated by green, yellow and red. However, the large residual strain at the iris provided a greater driving force for recovery and recrystallization, which can account for the more dramatic color change for the iris specimens after heat treatment. Furthermore, high LAM values are located near the surface region except around the grain boundary for the equator, while for the iris, large LAM values are present even in the bulk.

The grain boundary shown on the first iris specimen in Figure 7 is not an original grain boundary prior to deformation. The corresponding LAM map suggests that it could be a grain boundary induced by deformation. Since the boundary has large LAM values as indicated by the red and white, it appears to be a result of polygonization [8], where a low-energy configuration of dislocations developed where dislocations are equally spaced and lined up with each other. This implies that a large bending strain occurred during deep drawing at the iris to cause an unbalanced population of dislocations of one sign to generate a low angle boundary. Also, there must have been enough driving force for dislocations to rearrange themselves at room temperature, or, a preexisting low angle boundary became a trap for dislocation accumulation that led to the formation of a sharp boundary.

Figure 9 shows the LAM histograms for all 6 scans before and after heat treatment. Before heat treatment, all iris scans have larger LAMs than the equator scans, which is consistent with the observed color differences in the LAM maps. Plus, heat treatment resulted in more dramatic changes in the iris than the equator, as all the LAM peaks for the iris scans have moved by a noticeable amount to the left. On the other hand, the peak positions for the equator scans have not changed much, even after the 1000 °C heat treatment. This inadequate recovery (removal of defect content) at the equator may account for why the equator is sometimes more susceptible to hot spots in cavity operations. This is also in line with the observations in [7], where a larger strain tends to lead to a more complete recovery of phonon peaks after heat treatment.

CONCLUSIONS

EBSD analyses on the iris and equator specimens indicate that the surface damage from deep drawing depends on crystal orientations, is different at the equator and iris, and is severe even in the bulk at the iris. The iris and equator responded differently to heat treatment due to their different internal stress and defect states. While the 800 °C/2hr may be sufficient for recrystallization to occur near the iris, a higher temperature seems to be necessary for the equator to achieve a similar degree of dislocation removal.

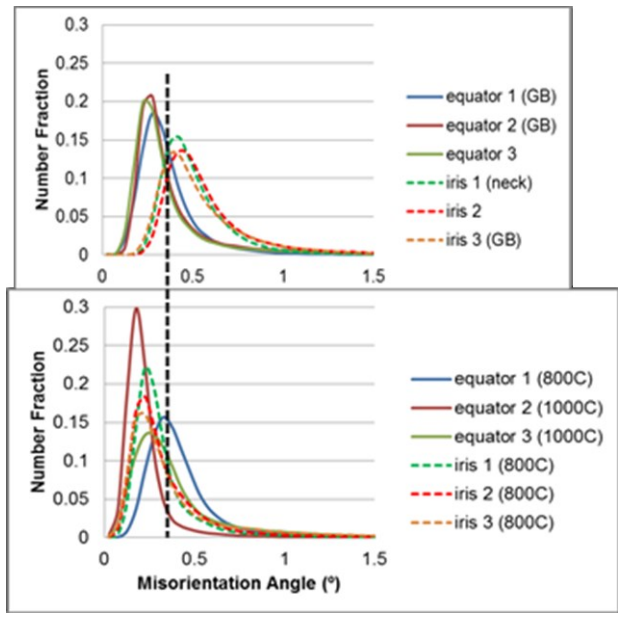

Figure 9: LAM histograms (summary view) for the 6 EBSD scans before and after heat treatment.

REFERENCES

[1] T. Bieler *et al*., Physical and mechanical metallurgy of high purity Nb for accelerator cavities, Physical Review Special Topics - Accelerators and Beams 13, 031002 (2010).

[2] H. Padamsee, RF Superconductivity: Science, Technology, and Applications (2009 WILEY-VCH Verlag GmbH & Co. KGaA, Weinheim).

[3] D. Baars, Investigation of active slip systems in high purity single crystal niobium, PhD dissertation.

[4] P. Kneisel, Performance of 1300 MHz KEK-Type Single-Cell Niobium Cavities, Proceedings of SRF97.

[5] G. Ciovati *et al*., AIP Conf. Proc. 1352, 25-37 (2011).

[6] S. Chandrasekaran *et al*., Effect of heat treatment temperature on thermal conductivity of large grain superconducting niobium, SRF2011.

ISBN 978-3-95450-143-4

[7] S. Chandrasekaran *et al.*, Recovery of phonon peak in annealed niobium as a function of initial strain and hydrogen concentration, SRFMW2012.
[8] D. Hull and D.J. Bacon, Introduction to Dislocations (Butterworth-Heinemann, Oxford, 2001), 4th Ed.
[9] L. Bortoloni - P. Cermelli, Statistically Stored Dislocations In Rate-Independent Plasticity, Rend. Sem. Mat. Univ. Pol. Torino Vol. 58, 1 (2000) Geom., Cont. and Micros., I.
[10] A. Romanenko, Review of high field Q-slope, surface measurements, Proceedings of SRF2007.
[11] EDAX/AMETEK, Inc., Introduction to Orientation Imaging Microscopy.
[12] EDAX-TSL Software V5.31 Manual.

ISBN 978-3-95450-143-4